VOL. 11, NO. 6, MARCH 2016 ISSN 1819-6608
ARPN Journal of Engineering and Applied Sciences

www.arpnjournals.com

INVESTIGATION OF MULTISPECTRAL IMAGING TECHNIQUE FOR OPTICAL MONITORING OF MEAN BLOOD OXYGEN SATURATION

Sheena P. Philimon, Audrey K. C. Huong and Xavier T. I. Ngu
Faculty of Electrical and Electronic Engineering, Universiti Tun Hussein Onn Malaysia, Batu Pahat, Johor, Malaysia
E-Mail: asheenaphil0210@gmail.com

ABSTRACT

This paper briefly reviews the feasibility of using multispectral imaging approach to noninvasively determine one's mean blood oxygen saturation, S_mO_2. We described the use of Extended Modified Lambert Beer (EMLB) model and a nonlinear fitting algorithm to quantitatively analyse the measured spectroscopic data over a wavelength range of 520-600 nm to give the best estimation of S_mO_2. The experimental work required spectroscopic images to be collected from the right index finger of four recruited volunteers at resting condition and after a pressure of 140 mmHg is applied on their upper right arm. The obtained results revealed a percent S_mO_2 of 77.5 ± 1.06% at resting condition and 54.3 ± 0.42% during blood flow occlusion. These results are also compared to that reported in previous works. The results show that these ranges and the drop in the mean percent S_mO_2 obtained for at rest compared to blood flow occlusion condition agreed considerably well with that reported in the literature. This work concluded that the developed multispectral imaging system could potentially be used as an alternative means to noninvasive monitoring and detection of changes in one's mean blood oxygen saturation with external interventions.

Keywords: extended modified lambert beer model, spectroscopy, multispectral imaging, mean blood oxygen saturation.

INTRODUCTION

The concept of near-infrared (NIR) spectroscopy has been a much discussed subject over the years and its application has been widely applied in various fields. One of the most notable uses of this system has been identified in the study of skin oximetry. Given the non-invasive attribute and the advantage at which the system is known to have no side risk, the concept of reflectance spectroscopy is highly opted for especially in the medical field and works involving biological specimens. The commonly available spectroscopic system are point spectroscopy, and its counterpart imaging spectroscopy namely hyperspectral imaging and multispectral imaging system. In a multispectral imaging system, an imaging sensor (i.e. Charge Coupled Detector (CCD) or Complementary Metal Oxide Semiconductor (CMOS)) produced distinguished spectroscopy images at multiple wavelengths obtained from the skin site of interest. These multiwavelength images are aligned accordingly to form a multispectral data cube which could provide spatial and spectral information (Bianco, Bruno, and Muzzupappa, 2013; Parmar, Lansel, and Wandell, 2008). Unlike the hyperspectral system that analysed hundreds to thousands of spectral band, the multispectral system analysed these spectrum at a relatively discrete and narrow band of less than 20 bands in each pixel produced (Freeman and Lewis, 2013). Hence, the hyperspectral system has a more complex computation that required longer processing time as compared to the latter.

In recent years, many researchers have acknowledged the use of reflectance spectroscopy to investigate tissue oxygenation and assess one's microcirculation health. These works vary in terms of data analysis and quantification method, wherein these works used either a library of data simulated using Monte Carlo method or diffusion model (Vogel *et al.*, 2007), or an analytical model such as Extended Modified Lambert Beer (EMLB) model (A. Huong and Ngu, 2014b), cumulant based attenuation model (A. K. C. Huong, 2012), cubic law (Kobayashi *et al.*, 2001) and a nonlinear fitting model (Pifferi *et al*., 1998) to quantitatively retrieve information on an individual's percent blood oxygen saturation, SO_2.

The objective of this study is to investigate the use of multispectral imaging to monitor one's blood oxygen saturation via Extended Modified Lambert Beer model developed by Huong and Ngu (A. Huong and Ngu, 2014a). Although the concentration of melanin and haemoglobin in the skin epidermis and dermal layer are most significant in the wavelength range of 520-600 nm, only the absorptivity of haemoglobin, HbO_2, and deoxyhaemoglobin, Hb, are considered in this study. This work assumes that a pressure of 140 mmHg applied on the upper arm of human subjects with mean systolic value of 120 mmHg is able to occlude arterial blood from flowing into the lower part of the corresponding arm.

This paper is organised as followed: the employed experimental setup and analytical model are described in Materials and Method section. This section also includes a brief description of iterative fitting procedure used to predict one's mean blood oxygen saturation, S_mO_2. This is followed by the findings of this work and a comparison of the results with that reported in the literature in the Results section. The final section discussed the obtained results and conclusion of this paper.

MATERIALS AND METHOD

Subjects and experimental procedure

Four Asian subjects consisting of both male and female, aged between 24-26 years old, were recruited in this study. The mean systolic and diastolic of these volunteers are measured at 120 mmHg and 78 mmHg, respectively. Prior to the measurements, the subjects were briefed on the experimental procedure and all volunteers gave their written informed consent. All these participants declared to be non-smokers with no serious underlying medical illness such as diabetes, anemia and pulmonary disease. This study begins with measurement at resting condition. First, the volunteers are acclimatized to room temperature for at least 15 minutes. Next, volunteers are required to sit in an upright position with their right hand placed lower than the heart level to allow unimpeded blood flow while multispectral reflectance images are taken at their right index finger. As for the arterial blood occlusion experiment, a cuff pressure of 140 mmHg is applied on their upper right arm for 60 seconds before measurement is taken from the right index finger of the respective subject. These experimental methods are chosen to verify the feasibility of using spectroscopic data collected from the developed multispectral imaging system to detect local changes in oxygenated blood flow under normal condition and during arterial blood occlusion.

Spectroscopic data acquisition system

In this present work, a cooled CCD camera (BUC4-500C Cooled CCD Digital Camera from BestScope) is used to capture the spectral images at intermediate wavelengths ranging between 520 − 600 nm with a spectral resolution of 10 nm. A high intensity light emitting diode (LED) (XLamp® XQ-E LED from Cree) is shone through the entrance slit of the monochromator (Oriel Mini Monochromator model 78026 from Newport) and dispersed from the exit slit to generate a spectrum between wavelength range of the monochromator (300-800 nm). A plano-covex lens (with diameter, Ø = 12.7 mm and focal length, f_L= 50.2 mm) is positioned in front of the CCD to form a principal focus point of the parallel reflected light, as shown in Figure-2. The targeted skin site is placed at a distance of 17 cm from the CCD. Due to the highly sensitive setup, this system is mounted on an optical table to reduce motion artefacts during image acquisition.

Image calibration and correction

The CCD camera used in the imaging system is adjusted with an exposure time of 5.71 seconds. This exposure time is selected to reduce the magnitude of noise signals considering the relatively low light source intensity and the low quantum efficiency (QE) of the employed CCD camera. These settings are controlled by the ISCapture application software (V3.5 from BestScope) which is installed along with the CCD camera and supported by Windows 7 operating system. The raw images are saved before it is analysed offline using MATLAB (MathWorks, Inc.).

In order to reduce the effect of dark noise signal on the image samples, image correction is performed by taking the dark reference data, which is acquired by covering the lens with a shutter cap. Meanwhile, the white reference given by the reflectance from a spectralon (from Labsphere, Inc.) with 99% reflectance is also taken for calculation of corrected light attenuation, $A_{corr}(\lambda)$ as follows:

$$A_{corr}(\lambda) = \frac{I_{white}(\lambda) - I_{dark}(\lambda)}{I_{sample}(\lambda) - I_{dark}(\lambda)} \quad (1)$$

where I_{sample}, I_{white} and I_{dark} denote wavelength dependent reflectance data of the human subject, white and dark reference, respectively.

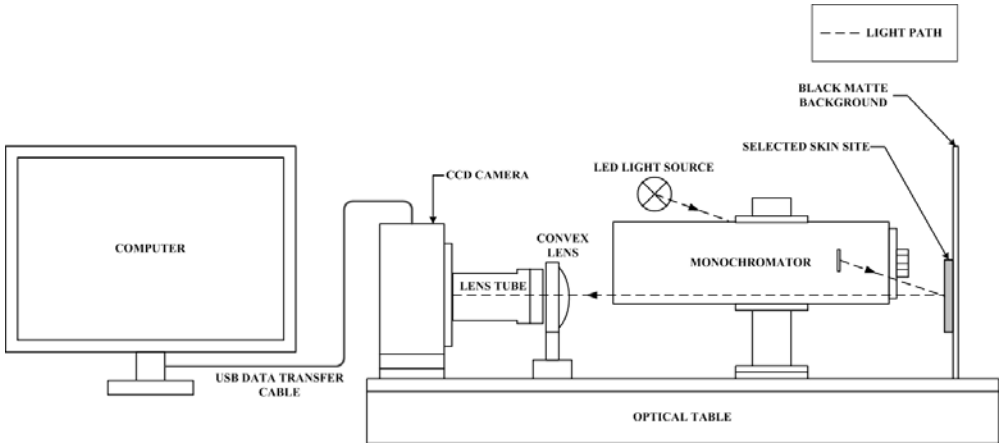

Figure-1. Schematic diagram of the multispectral imaging system (side view).

Extended modified lambert beer model

This work employed the EMLB model developed by Huong and Ngu (A. Huong and Ngu, 2014a) to determine the fractional concentration of oxyhaemoglobin in blood by means of a nonlinear fitting algorithm. The EMLB model is given by:

$$A(\lambda) = G_0 + \mu_a d_0 + G_1\lambda + \lambda \exp(-\mu_a d_1) \quad (2)$$

where:

$\mu_a(\lambda)$ = wavelength dependent light absorption
G_0 = light attenuation offset
d_0 = light path-length
$G_1\lambda$ = light attenuation due to epidermal absorption and scattering process

The exponential function in equation (2) delineates the expression of the light attenuation as a complex function of dermal light scattering and absorption in the dermis layer. Meanwhile, the total light absorption, μ_a is given as the sum of product of concentration, C, and wavelength dependent extinction coefficient, $\varepsilon(\lambda)$ given by:

$$\mu_a = \varepsilon_{HbO_2}(\lambda) C_{HbO_2} + \varepsilon_{Hb}(\lambda) C_{Hb} \quad (3)$$

Since this work assumes HbO_2 and Hb are the only absorbing medium in the dermis layer, the total haemoglobin concentration is defined as $T = C_{HbO_2} + C_{Hb}$. Substituting T into equation (3) gives μ_a expressed as:

$$\mu_a = \left(\varepsilon_{HbO_2}(\lambda) - \varepsilon_{Hb}(\lambda)\right) C_{HbO_2} + \varepsilon_{Hb}(\lambda) T \quad (4)$$

The percent S_mO_2 is expressed as a function of T as:

$$S_mO_2 = \frac{C_{HbO_2}}{T} \quad (5)$$

Hence, equation (4) can be rearranged to give:

$$\mu_a = \left(\left(\varepsilon_{HbO_2}(\lambda) - \varepsilon_{Hb}(\lambda)\right) S_mO_2 + \varepsilon_{Hb}(\lambda)\right) T \quad (6)$$

The EMLB model in equation (2) can further be expressed as:

$$A(\lambda) = G_0 + \left(\Delta\varepsilon S_mO_2 + \varepsilon_{Hb}(\lambda)\right) d_0 T + G_1\lambda + \lambda \exp\left(-\left(\Delta\varepsilon S_mO_2 + \varepsilon_{Hb}(\lambda)\right) d_1 T\right) \quad (7)$$

where $\Delta\varepsilon$ represents $\varepsilon_{HbO_2}(\lambda) - \varepsilon_{Hb}(\lambda)$.

Iterative fitting procedure

The measured attenuation data from the multispectral system is compiled and arranged as a stack of data prior to data analysis using an iterative fitting routine written in MATLAB. The best guess of S_mO_2 is searched via *fminsearch* function available in MATLAB. The algorithm is executed by first assigning all linear and nonlinear parameters (i.e. S_mO_2, G_0, d_0T, G_1 and d_1T) in equation (7) with an initial value of 1. This function applies an unconstrained nonlinear optimization method to iteratively seek the new value for the fitting parameters based on the size of error between the attenuated value given from the EMLB model and the measured attenuation value, ΔE. The fitting process is terminated when the absolute mean of ΔE value is less than 1×10^{-12} or when the number of iteration has achieved 1000, in which the optimum value of S_mO_2 is assumed to have been achieved.

RESULTS

Figure-2 shows multispectral image stack of right index finger of one of the volunteers collected over a selection of visible wavelength ranging between 520 nm and 600 nm with an interval of 10 nm. Each image shown in Figure-2 (on the left) is a spectral image, hence giving the spatial resolution and spectral resolution of the image. The distribution of intensity spectra is indicated by a colour bar. These images are then run in MATLAB software for calculation of light attenuation expressed in equation (1).

The calculated attenuation data is fitted using the EMLB model to give the best estimation of S_mO_2. The S_mO_2 value of the four individuals (identified as volunteer A, B, C and D) at resting condition and during arterial blood occlusion is calculated and the results are as shown in Table-1. The data collected using multispectral approach revealed an overall mean S_mO_2 of 77.5% and 56.2% at resting condition and during occlusion, respectively.

Since there is currently no specific standard to which the results can be compared to and the currently available pulse oximeter is only able to give measurement on arterial blood oxygen saturation, these results are compared with those previously reported in the literature, as tabulated in Table-2.

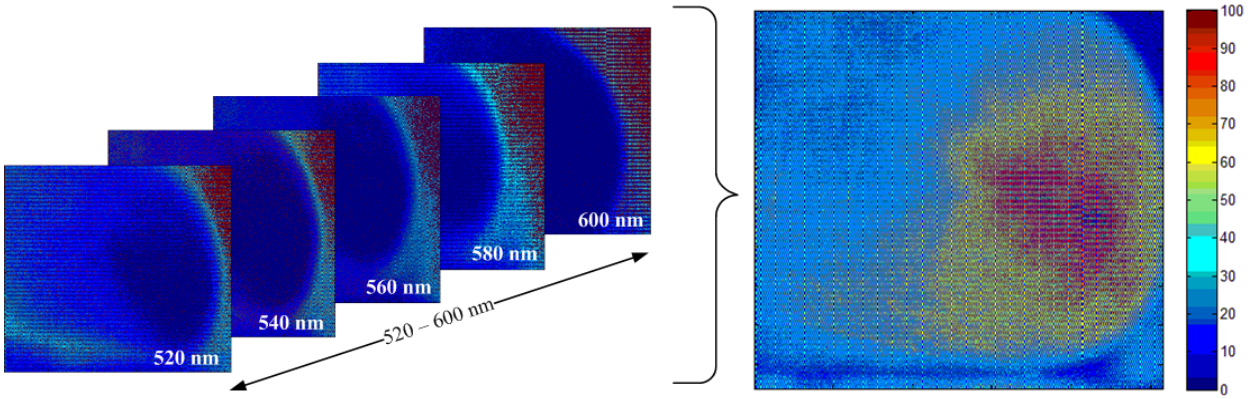

Figure-2. Multispectral data captured over a range of selected wavelength value aligned as a stack (left). The mean blood oxygen saturation, S_mO_2, of the selected skin site estimated from the collected multispectral images (right).

Table-1. Mean and standard deviation of mean blood oxygen saturation, S_mO_2, collected from the index finger of recruited individuals using multispectral imaging at resting condition and during arterial blood occlusion experiment.

Volunteer	Reported S_mO_2	
	At rest	Arterial blood occlusion
A	**76.8 ± 1.21%**	**56.6 ± 0.42%**
B	74.6 ± 1.18%	46.2 ± 0.64%
C	78.7 ± 1%	59.58 ± 0.38%
D	79.7 ± 0.83	54.7 ± 0.23%

Table-2. A comparison of mean blood oxygen saturation, S_mO_2, at resting and during arterial blood occlusion condition estimated in this study and in other previous related works.

Experimental Method	Analytical model	Reported mean blood oxygen saturation, S_mO_2	
		At resting condition	Arterial blood occlusion
This work	Fitting via EMLB model (multispectral imaging system)	77.5 ± 1.06%	54.3 ± 0.42%
Huong and Ngu (A. K. Huong & Ngu, 2015)	Fitting via EMLB model (point spectroscopy system)	94.5 ± 2.19%	56.76 ± 5.8%
Kobayshi *et al*. (Kobayashi *et al*., 2001)	Cubic function	68 ± 6%	48%
Vogel *et al*. (Vogel *et al*., 2007)	Power law model	50%	35%
Huong (A. K. C. Huong, 2012)	Improved linear equation and nonlinear fitting model, Gradient processing technique	74 ± 7%	33 ± 3%

DISCUSSIONS

The results shown in Table-1 revealed distinctive changes in the local distribution of HbO_2 from mean S_mO_2 of 77.5% at resting condition to 54.3% during arterial blood occlusion. This shows that the developed system and analytical technique are able to detect changes in one's S_mO_2 with a variation in their microcirculatory system. The calculated S_mO_2 value at resting condition agreed relatively well with that reported by Huong (A. K. C. Huong, 2012) that employed hyperspectral imaging system. There is, however, a variation of this value during blood occlusion experiment. This is likely due to differences in the pressure applied in the corresponding work compared to that used in this study.

Meanwhile, Kobayashi *et al*. (Kobayashi *et al*., 2001) and Vogel *et al*. (Vogel *et al*., 2007) reported a

slightly lower reading of blood oxygen saturation compared to that reported in the present study. A possible explanation for this is the inappropriate assumption of skin thickness and light propagation and scattering across different skin layers as discussed by Huong and Ngu (A. K. Huong and Ngu, 2015). It is important to note that during spontaneous arterial vasomotion, the surrounding tissue experienced an increase in the blood volume and a decrease in the distribution of HbO_2, this fact is supported by previous researches (Kamshilin *et al.*, 2013; Vogel *et al.*, 2007). These readings, however, are often concealed under low blood oxygen saturation and poor blood perfusion condition using a finger pulse oximeter, which detects mostly plasma in blocked microcirculatory tissue (Al-Ali, 2014).

It must be mentioned that the results obtained in this study substantially varied with the measurements conducted by Huong and Ngu (A. K. Huong and Ngu, 2015) using point spectroscopy in Table-2, wherein the corresponding work revealed a higher calculated mean S_mO_2 value of 94.5% and 56.76% at resting condition and with pressure applied, respectively. The corresponding authors argued that high S_mO_2 (with a value close to 100%) should be expected at fingertips due to the presence of arteriovenous anastomoses (AVAs). These AVAs permit direct shunting of arterial blood into the venous compartment (Thorn *et al*., 2009). In contrast to the point spectroscopy system where measurements are taken at proximal distance, in the present work selected skin site is placed at approximately 17 cm from the CCD detector in the multispectral system. This would subsequently degrade the spatial resolution of the collected images. An advantage of the multispectral system is, however, the possibility of using the CCD camera to allow a larger view of selected skin sites. This enables different skin optical properties to be retrieved via image acquisition and analysis. This is important especially to monitor differences in S_mO_2 of the wound sites and its surrounding tissues. The changes in S_mO_2 may then be used as an indicator to wound healing progress.

CONCLUSIONS

In this work, we observed changes in S_mO_2 reading with different experimental methods using multispectral imaging measurements performed on the right index finger of four volunteers. This shows the feasibility of using this system for noncontact and noninvasive monitoring of one's S_mO_2. This work concludes that the developed strategy can be used as an alternative mean to detect changes in one's blood oxygen saturation with external interventions.

ACKNOWLEDGEMENT

The authors would like to thank all volunteers who participated in this study. This research is funded by Universiti Tun Hussein Onn Malaysia (under MDR grant no. 1110, GIPS grant U165) and the Ministry of Education Malaysia (under RAGS grant no. R015 and R016).

REFERENCES

Al-Ali, A. 2014. Patient monitor for determining microcirculation state: Google Patents.

Bianco, G., Bruno, F. and Muzzupappa, M. 2013. Multispectral data cube acquisition of aligned images for document analysis by means of a filter-wheel camera provided with focus control. Journal of Cultural Heritage, 14(3), 190-200.

Freeman, J. E. and Lewis, E. N. 2013. Multispectral/hyperspectral medical instrument: Google Patents.

Huong, A. and Ngu, X. 2014a. The application of extended modified Lambert Beer model for measurement of blood carboxyhemoglobin and oxyhemoglobin saturation. Journal of Innovative Optical Health Sciences, 7(03).

Huong, A. and Ngu, X. 2014b. Noninvasive diagnosis of carbon monoxide poisoning using Extended Modified Lambert Beer Model. Paper presented at the 2nd International Conference on Electronic Design (ICED), 2014.

Huong, A. K. and Ngu, X. T. 2015. In situ monitoring of mean blood oxygen saturation using Extended Modified Lambert Beer model. Biomedical Engineering: Applications, Basis and Communications, 27(01), 1550004.

Huong, A. K. C. 2012. Spectroscopic analysis of scattering media via different quantification techniques. (Thesis), University of Nottingham.

Kamshilin, A. A., Teplov, V., Nippolainen, E., Miridonov, S. and Giniatullin, R. 2013. Variability of microcirculation detected by blood pulsation imaging. PloS one, 8(2), e57117.

Kobayashi, M., Ito, Y., Sakauchi, N., Oda, I., Konishi, I. and Tsunazawa, Y. 2001. Analysis of nonlinear relation for skin hemoglobin imaging. Optics Express, 9(13), 802-812.

Parmar, M., Lansel, S. and Wandell, B. A. 2008. Spatio-spectral reconstruction of the multispectral datacube using sparse recovery. Paper presented at the 15th IEEE International Conference on Image Processing, 2008. ICIP 2008.

Pifferi, A., Taroni, P., Valentini, G. and Andersson-Engels, S. 1998. Real-time method for fitting time-

resolved reflectance and transmittance measurements with a Monte Carlo model. Applied optics, 37(13), 2774-2780.

Thorn, C. E., Matcher, S. J., Meglinski, I. V. and Shore, A. C. 2009. Is mean blood saturation a useful marker of tissue oxygenation? American Journal of Physiology-Heart and Circulatory Physiology, 296(5), H1289-H1295.

Vogel, A., Chernomordik, V. V., Demos, S. G., Pursley, R., Little, R. F., Tao, Y., Gandjbakhche, A. H., Yarchoan, R., Riley, J. D. and Hassan, M. 2007. Using noninvasive multispectral imaging to quantitatively assess tissue vasculature. Journal of biomedical optics, 12(5), 051604-051604-051613.